# Development of a Printable Six-Axis Robot with Embedded Control for Cold-Plasma Wound Therapy


Aayushya Patel

Mentor: Sohail H. Zaidi


## Project Statement

Chronic wounds **affect ~40 million Americans annually**, costing **$25 billion in Medicare** expenditures. Cold atmospheric plasma (CAP) therapy, delivered via dielectric barrier discharge (DBD), has demonstrated up to **49% accelerated wound closure** in randomized trials; yet **clinical adoption remains stalled by operator-dependent manual delivery,** introducing non-uniform dosimetry, contamination risk, and safety hazards.

This project presents a fully custom-built **6-DOF robotic arm developed** from first principles to autonomously deliver DBD plasma along precise, **precomputed G-code tool paths** over arbitrary wound surfaces. The system integrates six closed-loop stepper actuators, **PETG 3D-printed structural joints,** a **custom PCB** with Teensy 4.1 with TMC5160 motor drivers, EMI-resistant cabling, LiDAR surface reconstruction, and an IR thermal-array safety interlock.

Mechanical validation over a 50 mm linear scan (n=50 positions, 0.5 kg payload) demonstrated mean **positional error of 0.027 mm** (max 0.069 mm), **100% of measurements below the 0.1 mm clinical threshold**. This platform provides the missing autonomous execution and standardization layer for research-grade plasma wound therapy.

## Background

**DBD plasma accelerates wound closure by up to 49%** in randomized trials. The **reactive oxygen and nitrogen species (RONS)** ($OH^-$, $O^-$, and $NO^-$) are the biologically active agents. RONS disrupt bacterial cell membranes and stimulate cellular proliferation for sterilization and tissue repair.

**Handheld CAP devices are fully operator-dependent**. **Inconsistent** standoff distance, speed, and coverage over complex wound geometries produce non-uniform dosimetry, **contamination risk**, and **safety hazards,** making manual delivery clinically inviable.

| System | DoF | Autonomous | Cost |
|---|---|---|---|
| Handheld DBD | N/A | No | ~$500 |
| Commercial Robotic Plasma | 6 | Partial | > $20,000 |
| Our Work | Autonomous toolpaths over arbitrary surfaces | Yes | ~$1000, Research Scale |

There is **no existing platform that combines sub-millimeter autonomous delivery, real-time wound mapping, and a research-accessible cost**, creating the gap this project directly addresses.

## Engineering Objectives

- Develop a 6-DOF robotic arm with sub-millimeter end-effector accuracy ***(Fig. 1)***
- Develop a multimodal sensor framework *(RealSense D405, MLX90640, spectroscopy, IR)* for real-time wound mapping and safety monitoring
- Develop a surface -to-G-code pipeline for autonomous, uniform plasma scanning ***(Fig. 8)***
- Validate RONS generation during operation via emission spectroscopy

| Criteria | Target | Result |
|---|---|---|
| End-effector Accuracy | < 0.10 mm | 0.027 mm mean, 0.069 mm max (50 mm scan, n=50, 0.5 kg payload) |
| Wound/Safety Sensing | RealSense + IR + spectroscopy integrated | All sensors operational; IR interlock enforces safe temp window |
| Surface-to-G-code | Autonomous toolpaths over arbitrary surfaces | Pipeline generates and executes G-code on reconstructed plane |
| RONS validation | Autonomous toolpaths over arbitrary surfaces | Spectra show expected RONS peaks |

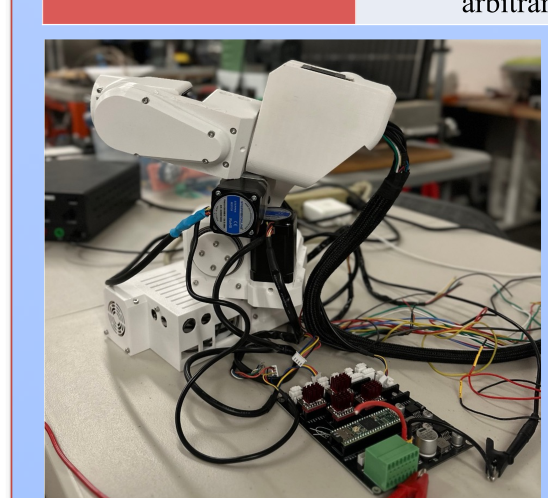

**Figure 1:** Final six-degree-of-freedom 3D-printed robotic arm platform used for autonomous plasma wound treatment

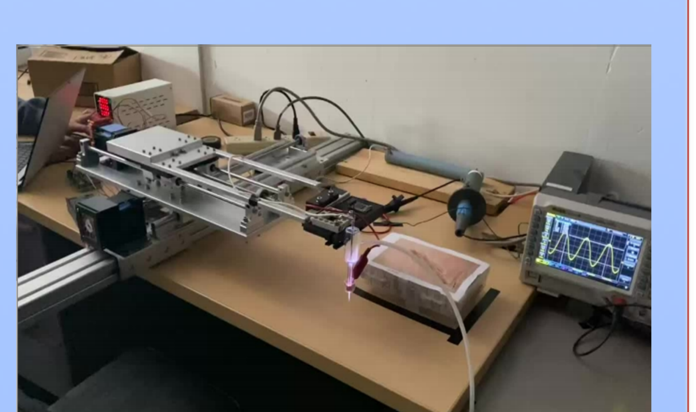

**Figure 2:** Early 2D prototype, operated with unshielded DBD plasma jet with open electrodes. Machine locked due to false microswitch triggers.

## Data

| Test | Expected (mm) | Measured (mm) | Error (mm) |
|---|---|---|---|
| 1 | 0.00 | 0.017 | 0.017 |
| 10 | 9.18 | 9.203 | 0.019 |
| 25 | 24.49 | 24.471 | 0.019 |
| 38 | 37.76 | 37.687 | 0.069 |
| 50 | 50.00 | 49.938 | 0.062 |

**Table 1:** Mechanical validation of the 6-DOF robotic arm over a 50 mm linear scan, showing expected vs. measured displacements that were recorded with precision calipers in a controlled setup; mean positioning error is 0.027 mm (max 0.069 mm, 100% pass <1mm).

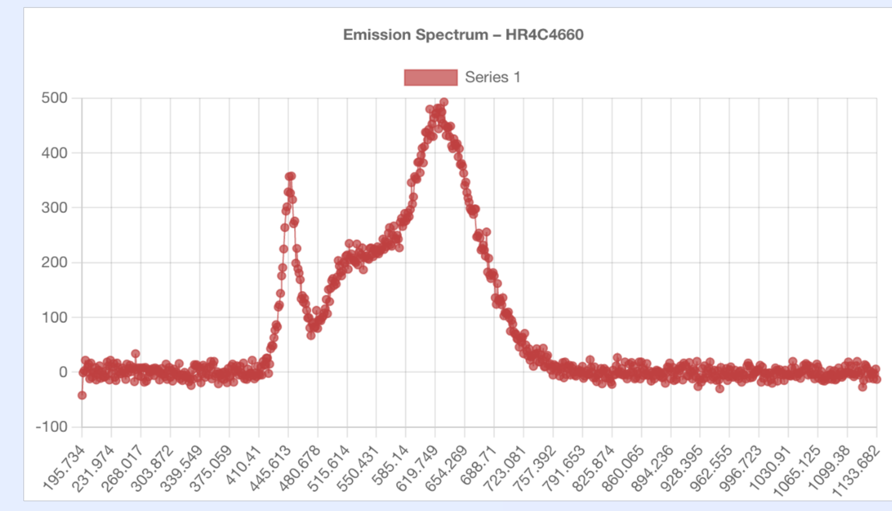


**Figure 3:** Optical emission spectrum of active DBD plasma jet (Ocean Optics HR4C4660, 195.7–1134.2 nm), showing characteristic discharge peaks consistent with the $N_2$ second positive system (300–500 nm) and OH emission bands, indicative of RONS generation.
<u>*Acquired via Ocean Optics HR4C4660 spectrometer (195.7–1134.2 nm range).*</u>

### Material Choice/FEA

PETG was chosen to be used in the robotic arm EMI control enclosures because of its very high resistivity (surface resistivity of 10 seventh of the square) and dielectric strength (16 kilovolt/millimeter) that enables passive isolation of EMI between the motor driver and control PCB (passive EMI). The design of parts was such that print orientation is optimized such that the stress loads are normal to the layer lines and the structural integrity is governed by continuous material, not inter-layer adhesion. PETG was the most suitable material due to its high layer bonding, chemical resistance and low cost which are essential in quicker, iterative enclosure prototyping without sacrificing the electromagnetic performance.

| | Tensile Strength | Tensile Modulus | Flexural Strength | Dielectric Strength |
|---|---|---|---|---|
| PETG | ~50 MPa (XY) | ~1,470 MPa | ~54 MPa | 16 kV/mm |

**Table 2.** Mechanical and dielectric properties of FDM-printed PETG used in robotic arm EMI control enclosure fabrication.

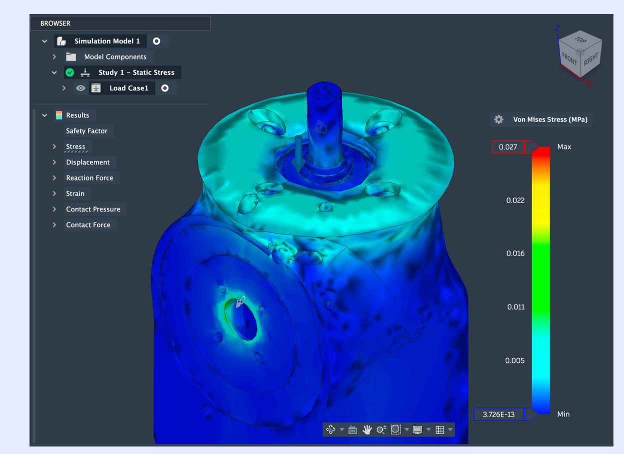


**Figure 4: Von Mises** stress distribution of the PETG EMI enclosure under static load (Fusion 360 FEA, Study 1), **well within PETG's tensile strength.** Stress concentration localized at the central mounting.

## Electronics Controller Architecture

A custom PCB was designed from scratch to integrate the six motor drivers (**TMC5160T Pro V1.0**), microcontroller for low level signal generation (**Teensy 4.1**), sensor integration, safety logic, and power safety control. The PCB schematic was first designed in EasyEDA Std, wires were then routed in their in-built PCB routing feature. PCB's were fabricated and assembled through JLCPCB with 4 layers. A silk screen was designed for part designation and orientation.

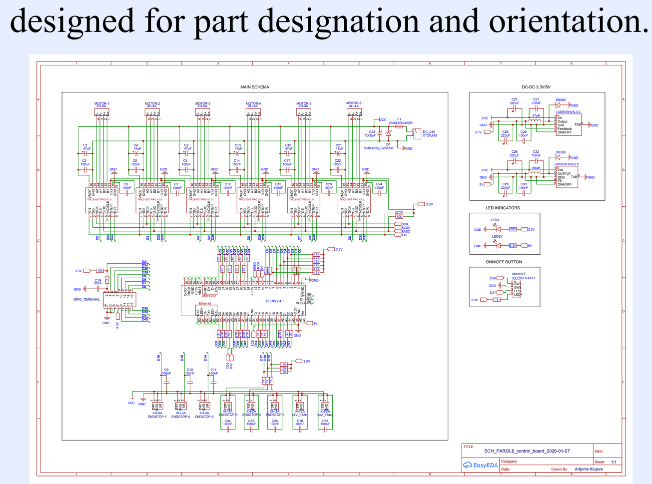

**Figure 5:** Custom PCB schematic integrating robotic control and sensing

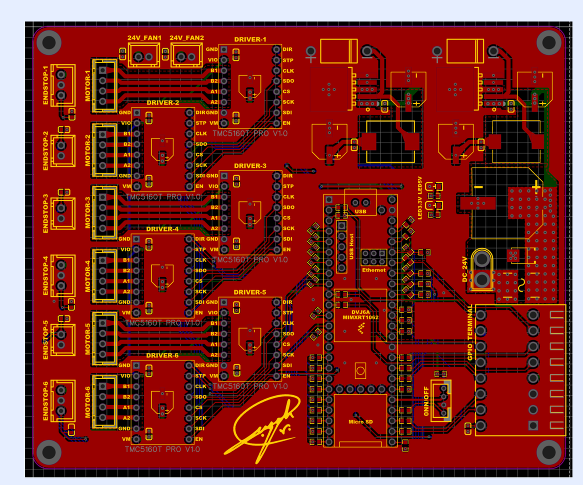

**Figure 6:** Final routed PCB layout used for robot operation. Deigned in EasyEDA

## Exploded View

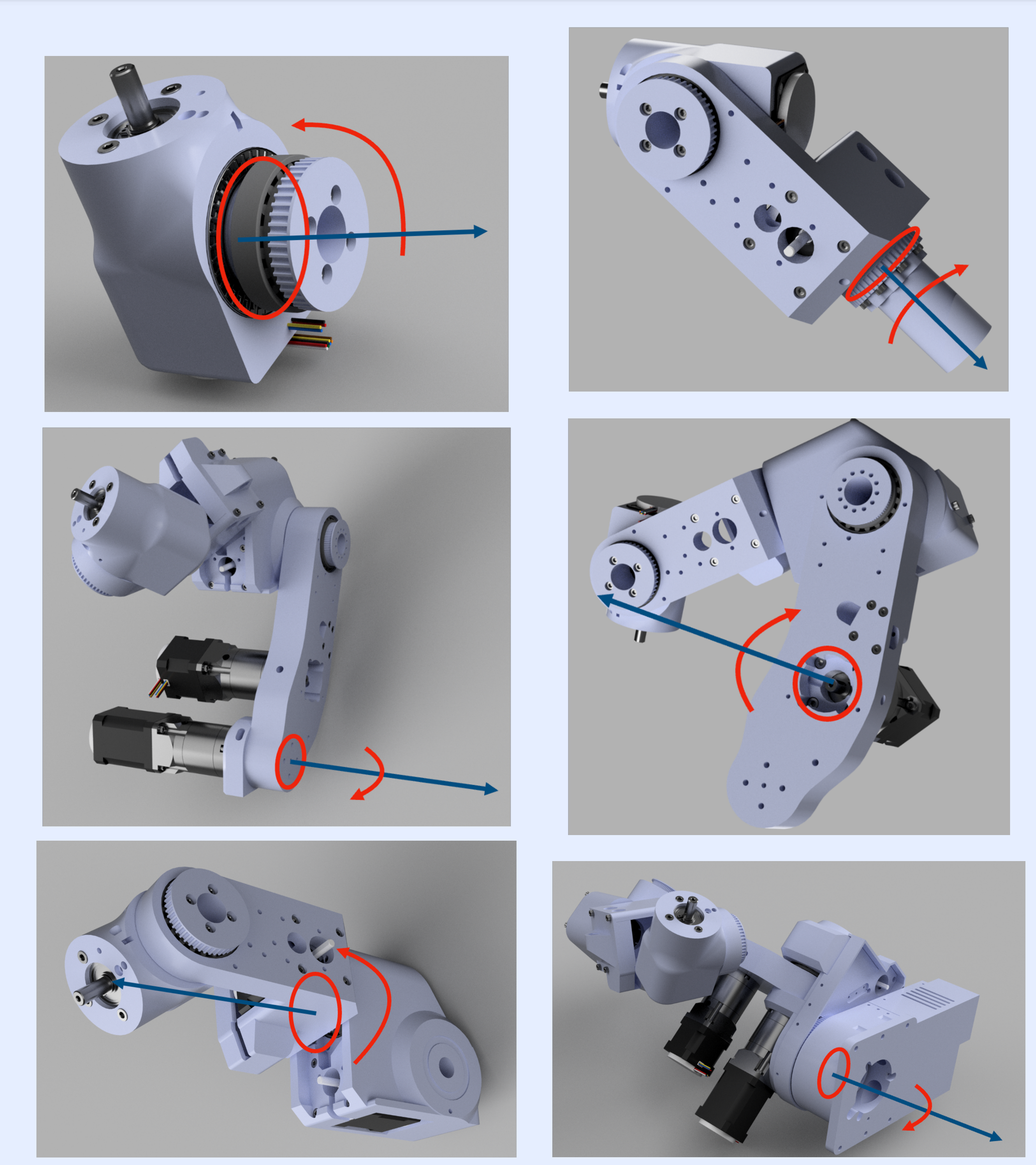

## Methods and Methodology

The system integrates a 6-DOF robotic arm ***(Fig. 1)*** with custom closed-loop motor control ***(Fig. 6)*** and a DBD plasma torch end-effector ***(Fig. 7)***. Four sensors, RealSense D405 (3D mapping), MLX90640 (thermal safety), HR4C4660 (RONS verification, Fig. 4), and IR reflective (distance control), provide real-time feedback to a safety arbiter that enforces thermal (<40°C) and distance (6–15 mm) limits before issuing motion commands.

The RealSense camera generates 3D point clouds of wound surfaces, which are processed to detect boundaries and generate G-code raster toolpaths ***(Fig. 8)***

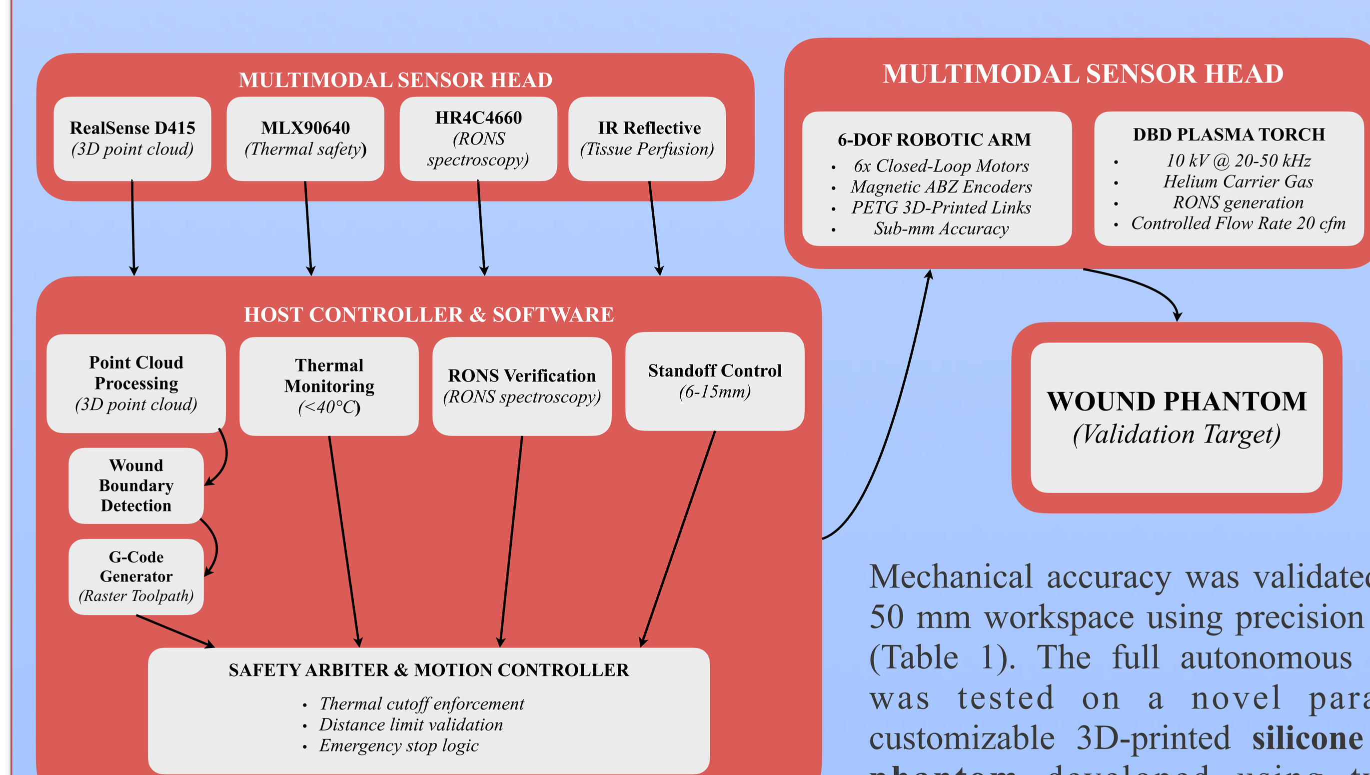


Mechanical accuracy was validated over a 50 mm workspace using precision calipers (Table 1). The full autonomous pipeline was tested on a novel parameter-customizable 3D-printed **silicone wound phantom** developed using two-part silicone elastomers.

| Joint | d (mm) | a (mm) | Theta offset |
|---|---|---|---|
| 1 – Base | 110.50 | 23.42 | 0 |
| 2 - Shoulder | 0 | 180.00 | -90 deg |
| 3 – Elbow | 0 | 43.50 | +180 deg |
| 4– Wrist 1 | 176.35 | 0 | 0 |
| 5 – Wrist 2 | 0 | 0 | 0 |
| 6 – Wrist 3 | 62.80 | 45.25 | +180 deg |

**Table 2:** Denavit–Hartenberg Parameters of the 6-DoF Robotic

## Results & Validation

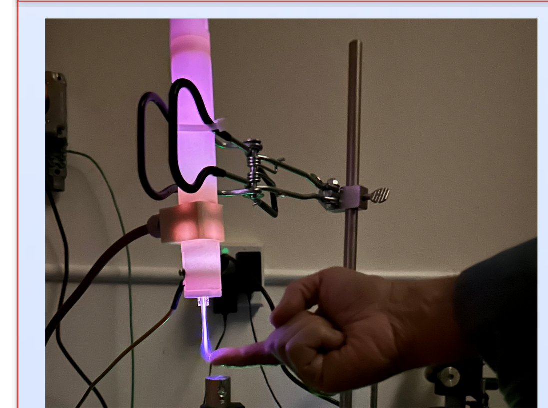

**Figure 7:** Custom DBD atmospheric plasma jet (10 kV, He carrier gas) generating a therapeutic ionized plasma plume for robotic end-effector deployment.

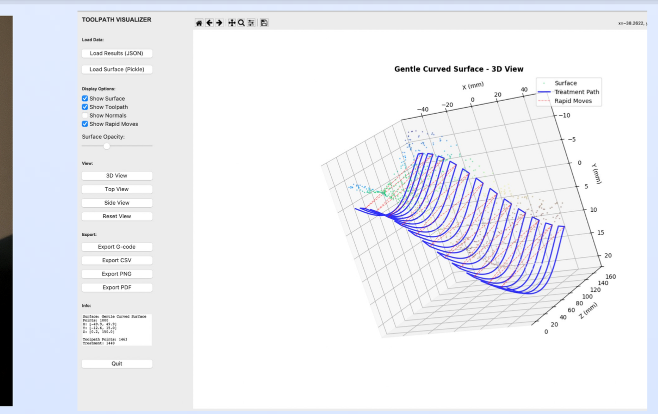

**Figure 8:** Custom toolpath rasterizer generating a scan treatment path (blue) over non-planar geometry. *1,443 points computed across a 160 × 120 mm surface.*

**Mechanical Performance**

**Positional accuracy:** 0.027 mm mean (max 0.069 mm, 100% pass <1 mm tolerance) ***(Table 1)***

Validated across 50 mm workspace using precision calipers

**Sensing & Plasma Verification**

**RealSense D405:** Real-time 3D wound surface mapping achieved

**MLX90640:** Thermal safety cutoff validated at 40°C (human tissue threshold)

**Spectroscopy:** RONS peaks confirmed at 300–500 nm during active plasma operation ***(Fig. 3)***

**Autonomous Scanning**

Full pipeline validated: point cloud → G-code → robotic motion → plasma delivery

Raster-pattern scanning successfully executed on wound phantom ***(Fig. 8)***

## Conclusions

- A fully functional 6-DOF robotic platform achieving **sub-millimeter** accuracy demonstrates the feasibility for a precise, autonomous plasma wound delivery system
- Multi-sensor integration *(3D vision, thermal, spectroscopy, distance)* addresses core limitations of manual delivery: **non-uniformity, unsafe dosing, and lack of reproducibility**
- At $869, this establishes a **low-cost research instrument** pathway toward standardizing plasma-based wound therapies in clinical settings

## Future Work

- Real-time spectroscopy feedback to adjust plasma parameters mid-scan
- Depth-aware path replanning for curved/irregular geometries
- Bacterial sterilization studies on culture plates
- Automated wound boundary detection from RealSense RGB+depth
- Safety protocol development for in-vivo wound models

## Selected References


1. Sen CK. Human Wound and Its Burden: Updated 2025 Compendium of Estimates. Adv Wound Care (New Rochelle). 2025.
2. Bekeschus S, et al. Medical gas plasma-stimulated wound healing: Evidence and mechanisms. Redox Biol. 2021.
3. Graves DB. The emerging role of reactive oxygen and nitrogen species in redox biology and some implications for plasma applications to medicine and biology. J Phys D Appl Phys. 2012
4. Isbary G, Morfill G, Zimmermann J, Shimizu T, Stolz W. Cold atmospheric plasma: a successful treatment of lesions in Hailey-Hailey disease. Arch Dermatol. 2011
5. Lu X, et al. Cold atmospheric plasma jet-generated RONS and their selective anticancer effects. Sci Rep. 2016
6. Patel A, Zaidi SH. Development of a 6-DOF Robotic Platform for Autonomous Plasma Wound Treatment. IEEE ISEC. 2026.